Non-Uniformly Charged Ionic Polymer-Metal Composite (IPMC) Actuators: Electromechanical Modeling and Experimental Validation

P.J. Costa Branco, B. Lopes, and J.A. Dente

***Abstract*— An IPMC composite is an electroactive material that behaves in an electric field similarly to biological muscles. This intelligent material is leading to a new emerging technology called non-uniformly charged IPMC actuators. This paper introduces first an IPMC analytical modeling approach for its electromechanical characterization. The model considers, for the first time, the action of gravitation force in its electric and mechanic characteristics, which is important for large IPMC actuators. To demonstrate the efficacy of the model, two non-uniformly charged IPMC actuators were fabricated and tested. Experimental results are presented to validate the model and verify its effectiveness in the design of non-uniformly charged IPMC actuators.**

***Index Terms*—Electric actuators, Ionic polymer-metal composites, IPMC, Intelligent materials, Polymers**

I. Introduction

Conventional actuators using electromagnetic forces [1] are still important in motion control. However, they have difficulty in satisfying the new and advanced demands from high performance machines [2], [3]. Therefore, seeking for innovative actuators [4] as shape memory alloy [5], magnetostrictive [6], and more recently IPMC actuators [7], [8], is today an intense research activity. IPMCs are functional materials [9] being electroactive polymers [10]–[11]. They are made by Nafion polymer electroplated with gold or platinum with negative sulfonates (SO_3^-) fixed to its structure.

The IPMC operates as actuator or sensor [12]. As sensor, it has to be subjected to an external mechanical pressure resulting in an electric current or voltage at its terminals. The IPMC has the disadvantage of needing an electrolyte for its operation, usually sodium electrolyte or ionic liquids [13]. The IPMC needs continuing hydration to avoid dryness problems which increase its stiffness and decrease its actuating/sensing capabilities. Two procedures were proposed to avoid IPMC dehydration: its encapsulation [14]–[15], or using an electrolyte with low evaporation constant [16]–[17]. When in sodium electrolyte, for example, the IPMC has water as solvent with Na^+ being the mobile ions. The IPMC conducts Na^+ across its membrane, showing its property of being permeable to them but not to Cl^-. Metal electrodes plated in the Nafion must be flexible and porous because the IPMC must be bendable, and porous because they must allow the passage of positive ions from the electrolyte to the polymer.

IPMC actuators can be commanded by voltage or current [18], [19]. Fig. 1(a) shows that when a voltage is applied to an IPMC, Na^+ ions are dislocated from positive to negative potential. This causes the appearing of an internal electric field acting on fixed negative ions and causing electrostatic forces transmitted to Nafion structure, causing an IPMC deformation.

Fig. 3(a) shows that during the electric process caused by an applied voltage, some positive ions come out of the IPMC through the negative electrode due to diffusion flow since electrodes are porous. Hence, since the internal negative ions' charge is not compensated with new positive ones, the IPMC suffers a so-called relaxation of its membrane and the IPMC returns to its steady position. If an electric current is applied instead a voltage, as in Fig. 1(b), the relaxation problem does not occur because the flux of positive charges is compensated continually. Applying an electric current, the positive ions will be in constant migration from outside to inside or inside to outside of the IPMC, keeping the flow of positive charges (charges that are balanced out with the entering positive charges), maintaining constant the electric force density in the IPMC. The authors previously published works [17] and [19] show a series of experimental results that illustrate the non-relaxation phenomenon when the IPMC is under current control.

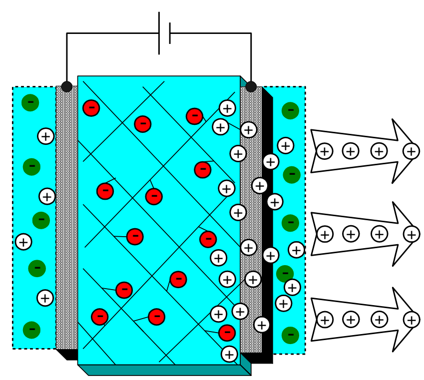

(a)

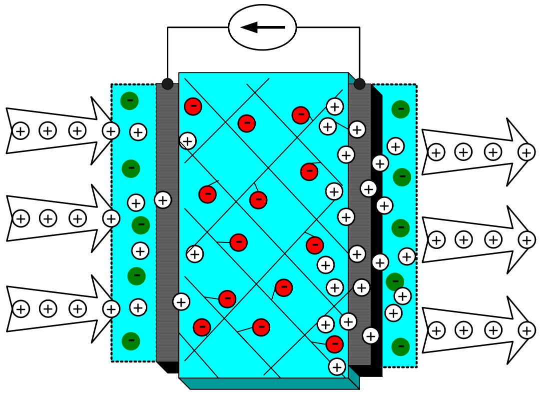

(b)

Fig. 1. (a) Voltage signal and (b) current signal applied to the IPMC.

The majority of current research on IPMC actuators is based on IPMCs that are completely covered with platinum electrodes, i.e., uniformly charged IPMCs. However, some recently research on no-uniformly covered IPMCs has appeared. Nakabo in [20] proposed a kinematic model of an IPMC based serial-link multi-DOF robot manipulators that instead of joint rotation, the link itself bends on an IPMC. Their modeling is a classical mechanic approach and does not incorporate any physical electromechanic phenomena occurring in the IPMC. Kim [21] and Dogruer [22] developed an analytical model of a segmented IPMC. However, the model proposed in this paper is more general since it can be applied to a segmented and non-segmented IPMC, even with large Nafion areas. Our segments did not need to be laser cut but one can deposit the electrode plates in a pre-defined area.

The model developed extends the authors' research in [19] and [24] by incorporating for the first time the effect of gravitation force in an IPMC electromechanical model, which will certainly influence the behavior of large IPMC actuators. When comparing with the more recent IPMC model proposed by McDaid in [23], our model takes an applied current and not voltage, and thus the back-relaxation phenomenon disappears.

In this paper, non-uniformly charged IPMC actuators, which have the advantage of using the higher elastic properties of the Nafion, are modeled. More specifically, non-uniformly charged IPMCs have some areas covered with electrodes and others not covered, containing only the Nafion polymer. The area covered with electrodes depends on the IPMC geometry chosen for a particular application. To obtain a non-uniformly charged IPMC, those areas where one wants to have only the Nafion are covered with a non-metallic layer as a dielectric gel. Therefore, when in the IPMC electrode plating, only those areas not covered with dielectric gel will react with the electrode metal layer.

The model is applied in the electromechanical characterization and analysis of two non-uniformly charged IPMC actuators. A set of experiments with the two actuators were conducted to validate the model in their design.

II. The IPMC Electromechanical Model

The IPMC model can be divided into two parts: the mechanical part, which takes into account the internal mechanic stresses due to internal pressures and also the electric forces inside the Nafion; and the second model part, the electrical one, which takes into account the positive ions electric current and the resultant electric field distribution inside the IPMC.

A. *The Mechanical Model*

The mechanical model is developed based on the assumption that the Nafion remains in its elastic property, and the model also assumes that the thickness of the IPMC is negligible, compared with its length. Fig. 2 represents an IPMC sheet and its coordinate axes. The IPMC length is *b*, the width is *l*, and *d* is the thickness.

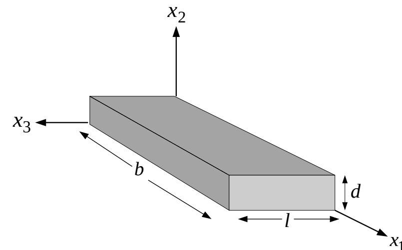

Fig. 2. IPMC sheet with its main dimensions.

Applying Newton's second law to a volume element of the IPMC, its dynamic can be approximated by

$$\rho\frac{\partial^2\delta_i}{\partial t^2}=F_i^{mec}+F_{ei}^-,\, i=1,3 \text{ and } \rho\frac{\partial^2\delta_2}{\partial t^2}=F_2^{mec}+F_{e2}^-+F_g,\, i=2 \quad (1)$$

where ρ is mass density, δ_i is the material displacement in direction i, F_i^{mec} is the mechanical force density, F_{ei}^- is the electric force density actuating in the negative ions (SO_3^-) fixed in the Nafion, and F_g is the gravitation force's density acting in $-x_2$ direction and given in (2) where g is the gravitation constant. The force density F_i^{mec} is caused by mechanical stresses T_{ij}^{mec} imposed on the volume element by the surrounding material, and is related with those stresses as indicated in (2).

$$F_g=-\rho g\,, \qquad F_i^{mec}=\frac{\partial T_{ij}^{mec}}{\partial x_j}.,\ j=1,2,3. \qquad (2)$$

From the theory that describes the motion of an isotropic elastic medium (see [25] and [26]), the expression for T_{ij}^{mec} in terms of material displacements δ is given by

$$T_{ij}^{mec}=2G\left(\frac{\partial\delta_i}{\partial x_j}\right)+\lambda\delta_{ij}\frac{\partial\delta_k}{\partial x_k},\, G=\frac{Y}{2(1+\upsilon)},\, \lambda=\frac{\upsilon Y}{(1+\upsilon)(1-2\upsilon)} \quad (3)$$

where G is the shear modulus, λ is the Lamé constant, Y is the IPMC elastic modulus and υ its Poisson's ratio. Term δ_{ij} in (3) is the Kronecker delta function [25].

Since we are assuming that there are no significant forces applied to the IPMC in x_3 direction, IPMC stresses T_{31}^{mec}, T_{32}^{mec}, T_{13}^{mec} and T_{23}^{mec} are null. Using these conditions in (1) results in two motion equations for the IPMC given by

$$\rho\frac{\partial^2\delta_1}{\partial t^2}=\frac{\partial T_{11}^{mec}}{\partial x_1}+\frac{\partial T_{12}^{mec}}{\partial x_2}, \qquad (4)$$

$$\rho\frac{\partial^2\delta_2}{\partial t^2}=\frac{\partial T_{21}^{mec}}{\partial x_1}+\frac{\partial T_{22}^{mec}}{\partial x_2}+F_{e2}^-+F_g, \qquad (5)$$

where any material displacement in direction x_3, i.e., δ_3, was neglected. For (4), F_{e1}^- was neglected because we consider the existence of electric forces only in direction x_2 due to IPMC be very thin when compared with its length.

The relation between material strain e_{ij} with material displacement δ is given in (6) [25]. For $i=j$ and $i\neq j$, strains e_{ij} are related with mechanical stresses as indicated in (6).

$$e_{ij} = \frac{1}{2}\left(\frac{\partial \delta_i}{\partial x_j} + \frac{\partial \delta_j}{\partial x_i}\right),\ e_{ii} = \frac{1}{Y}\left[T_{ii} - \upsilon\left(T_{jj} + T_{kk}\right)\right],\ e_{ij} = \frac{T_{ij}}{2G} \quad (6)$$

Taking into account the conditions previously applied to IPMC stresses, (6) results in (7).

$$e_{11} = \frac{\partial \delta_1}{\partial x_1} = \frac{1}{Y}\left[T_{11}^{mec}\right],\ e_{22} = \frac{\partial \delta_2}{\partial x_2} = \frac{1}{Y}\left[-\upsilon T_{11}^{mec}\right],\ e_{33} = \frac{\partial \delta_3}{\partial x_3} = 0 \quad (7)$$

Our objective now is to obtain the motion equations for the longitudinal δ_1 and transverse IPMC displacement δ_2. Due to the small thickness of the IPMC, its behavior can be approximated with a one-dimensional model because the material displacement in direction x_1 is minor ($\delta_1 \approx 0$). All details of how this model is obtained are given in [19]. Here, we only give the final motion equation (8) with the gravitation force included.

$$\rho \frac{\partial^2 \delta_2}{\partial t^2} = \frac{1}{2}\left(x_2^2 - \left(\frac{d}{2}\right)^2\right) Y \frac{\partial^4 \xi}{\partial x_1^4} + \left[(2G+\lambda)\upsilon - \lambda\right]\frac{\partial^2 \xi}{\partial x_1^2} + F_{e2}^- - \rho g. \quad (8)$$

In this equation, force density F_{e2}^- will be determined from the IPMC electrical model developed next.

B. The Electrical Model

The electrical model assumes the IPMC made by three species: mobile positive ions, fixed negative ions, and water molecules. We take into account that sulfonate ions are chemically fixed to Nafion structure, and the resultant force experienced by them is null. Hence, only the positive ions and water molecules will be significant for IPMC electrical model.

Because water molecules have a higher density mass than the positive ions ($\rho^h >> \rho^+$), and also since the positive ions speed is assumed greater than water molecules ($v^+ >> v^h$), momentum equations of the ion and water species yield

$$\frac{d(\rho^+ v^+)}{dt} = \mathbf{F}^+ = 0\ ,\ \frac{d(\rho^h v^h)}{dt} = \mathbf{F}^h = 0\,. \quad (9)$$

1) *Positive Ions:* The total force density $\mathbf{F}^+$ acting on the positive ions is given by:

$$\mathbf{F}^+ = F_e^+ + F_d^+ + F_p^+ + F_u^+ + F_g^{\ +} \quad (10)$$

where F_e^+ is the electrostatic force density, F_d^+ is the force density due to diffusion process, F_p^+ is the force density due to the space variation of mechanical stresses acting on positive ions, F_μ^+ is the friction force density applied to positive ions by water molecules, and F_g^+ is the gravitation force´s density.

Electrostatic force (F_e^+): The electrostatic force density is:

$$F_e^+ = \rho_c^+ E \quad (11)$$

where ρ_c^+ is the electric charge density of positive ions [C/m^3] and E is the electric field strength [V/m].

Diffusion force (F_d^+): Initially, the positive ions are concentrated in the outer surface of the IPMC. The effect of mass diffusion due to concentration differences makes positive ions penetrate the IPMC where they are in lower concentration. Variable C_s is the molar concentration, which gives us the relationship between mass densities of positive ions and water molecules:

$$C_s = \frac{\rho^+}{\rho^+ + \rho^h} = \frac{\rho^+}{\rho}\,. \quad (12)$$

The diffusion force F_d^+ given in (13) is obtained by the gradient of a chemical potential μ in a chemical field [27]. The unit of F_d^+ is N/mol, T is temperature in Kelvin, and R is the gas constant.

$$F_d^+ = -\nabla\mu = -\frac{RT\rho^+}{C_s}\nabla C_s = RT\left[\left(\frac{\rho^+}{\rho}\right)\nabla\rho^h - \left(\frac{\rho^h}{\rho}\right)\nabla\rho^+\right] \quad (13)$$

Since the water mass density is constant, $\nabla\rho^h = 0$, and knowing that $\rho^h >> \rho^+$, (13) is approximated to (14).

$$F_d^+ = RT[-\nabla\rho^+]\,. \quad (14)$$

Mechanical force (F_p^+): The IPMC mechanical forces are determined by the gradient of internal pressures exerted on each adjacent elementary volume. Hence,

$$F_p^+ = -\nabla p_{mec} \quad (15)$$

The pressure gradient term ∇p_{mec} is equal to the total mechanical force density in direction x_2 and becomes given by (16) as detailed in [19].

$$F_p^+ = -\left[\frac{1}{2}(x_2^2 - (d/2)^2)Y\frac{\partial^4\xi}{\partial x_1^4} + \left[(2G+\lambda)\upsilon - \lambda\right]\frac{\partial^2\xi}{\partial x_1^2}\right]. \quad (16)$$

Friction forces (F_μ^+): Water molecules have a mass density much higher than that of positive ions, causing different propagation velocities and thus the appearance of friction forces between water molecules and ions, which are proportional to their speed difference as:

$$F_u^+ = -\eta(v^+ - v^h) \quad (17)$$

where η is a friction constant, $\eta = K\rho^+$, which is proportional to the mass density of the positive ions. Assuming that the speed of the positive ions is much greater than the speed of the water molecules, yields for the friction force:

$$F_u^+ \cong -K\rho^+ v^+\,. \quad (18)$$

Gravitation force (F_q^+): Gravitation force´s density is given by (19) where ρ is IPMC mass density after immersion in electrolyte, i.e., after absorption of water molecules and positive ions.

$$F_g^{\ +} = -\rho g \quad (19)$$

2) *Positive Ions Density Current* (J^+)*:* In the absence of significant effects of acceleration, the total force density on the positive ions is assumed to be in equilibrium. That is:

$$F_e^+ + F_d^+ + F_p^+ + F_u^+ + F_g = 0 \quad (20)$$

Using (11 - 19) into (20) results in J^+ expressed as

$$J^{+}=\left(\frac{\rho_c^{+}q^{+}}{Kp}\right)E-\left(\frac{RT}{K}\right)\nabla\rho_c^{+}-\left(\frac{q^{+}}{Kp}\right)\nabla p_{mec}+\left(\frac{q^{+}}{Kp}\right)\rho g\ , \tag{21}$$

knowing that the relationship between the electric charge density and mass density of the positive ions is given by

$$\rho^{+}=\frac{p}{q^{+}}\rho_c^{+} \tag{22}$$

where p is the ion weight and q^{+} is the ion electric charge. First right term in (21) represents the electrical conductivity σ, which determines the Joule losses in the IPMC. When compared with other terms, this can be neglected. A diffusion coefficient (23) is related to the absorption of positive ions by the IPMC. An L_p parameter is defined as (24). This parameter is related to the intensity of the force that the IPMC can develop, that is, the higher the value of L_p, the greater are the IPMC internal density forces [17].

$$D_f=\frac{RT}{K} \tag{23}$$

$$L_p=\frac{q^{+}}{Kp}\ . \tag{24}$$

Substituting (23)–(24) into (21), ion current density reduces to the form:

$$J^{+}\cong-D_f\nabla\rho_c^{+}-L_p(\nabla p_{mec}-\rho g)\ . \tag{25}$$

From (25), it can be argued that the diffusion process, the difference between mechanical stresses, and the gravitational density force, are the main phenomena related to the appearance of a positive ionic current inside the IPMC.

3) *Electric Charge Density of Positive Ions*: Considering that, $\nabla\cdot J^{+}=0$, Eq. (25) yields:

$$-D_f\nabla^2\rho_c^{+}-L_p\nabla^2 p_{mec}=0\ . \tag{26}$$

According to (26), gravity will not influence the distribution of positive ions. Solving Eq. (26), as detailed in [19], gives the ionic charge density of positive ions (27) where Q is the electrical charge at the IPMC surfaces.

$$\rho_c^{+}=\frac{8Qx_2}{d^2bl}-\rho_c^{-} \tag{27}$$

4) *The Electric Field Distribution in the IPMC*: We neglected edge effects, i.e., it was considered that electric field lines have only direction x_2. The electric field and electric displacement can be written as

$$E=-E_2(x_2,t)\mathbf{i}_2\ ,\qquad D=-D_2(x_2,t)\mathbf{i}_2\ . \tag{28}$$

From $\nabla\cdot D=(\rho_c^{+}+\rho_c^{-})$ and using (27) results in (29).

$$E_2(x_2)=\frac{2Q(d^2-2x_2^2)}{d^2bl\varepsilon}\ . \tag{29}$$

The IPMC voltage is the integral of (29) along IPMC thickness. The result, (30), is the relationship between electric charge Q and IPMC voltage.

$$Q=\frac{3}{5}\frac{\varepsilon bl}{d}V\ . \tag{30}$$

5) *The Electric Force Density*: The electric force density is expressed by $F_{e2}^{-}=(\rho_c^{+}+\rho_c^{-})E_2$. Using (29) gives (31).

$$F_{e2}^{-}=\frac{16Q^2x_2(d^2-2x_2^2)}{d^4b^2l^2\varepsilon}\ . \tag{31}$$

C. The IPMC Electromechanical Model

Integrating (8) through the IPMC cross section, using (30) and (31), results in (32) where ΔT_2 is pressure applied between IPMC surfaces.

$$\frac{\partial^2\xi}{\partial t^2}+Y\frac{d^2}{12}\frac{\partial^4\xi}{\rho\partial x_1^4}=\frac{\Delta T_2}{\rho d}+\frac{27}{50}\frac{\varepsilon l V^2}{\rho d^3}-g\ . \tag{32}$$

1) *Operation in Steady-State Regime*: Solving (32) in steady-state regime, we obtain the equation of the transverse displacement of the IPMC as:

$$\xi(x_1)=\left[\frac{1}{2Yd^3}\Delta T_2+\frac{27}{100}\left(\frac{\varepsilon l}{Yd^5}V^2\right)-\frac{1}{2Yd^2}\rho g\right]x_1^4+ +\frac{C_1x_1^3}{6}+\frac{C_2x_1^2}{2}+C_3x_1+C_4\ , \tag{33}$$

where the constants have to be obtained from the boundary conditions of the IPMC actuator.

III. Non-Uniformly Charged IPMC Actuators: Model Validation

A. The Experimental Setup

Fig. 3 shows the setup used in our tests. A non-uniformly charged IPMC actuator is hydrated using propylene-Li^{+} electrolyte. The IPMC is clamped at both ends and subject to current excitation generated from a commanded current power source. A Baumer laser position (±0.02 mm) measures the IPMC displacement through its length using a roller.

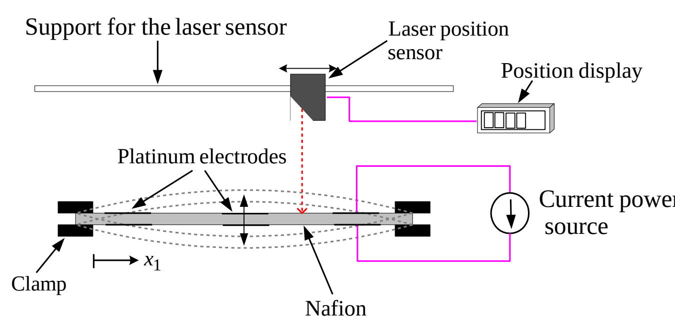

Fig. 3 Experimental setup for the IPMC tests.

B. Electromechanical Model Validation

In this section, two non-uniformly charged IPMC actuators are exhibited and used to validate the electromechanical model considering the effects of gravity. Tables I and II list the IPMC model parameters [19]. The IPMC actuators used in this paper were obtained from Environmental Robots Inc.

Table I.
Electrical parameters of the IPMC.

F(C mol^{-1})	ρ_c^{-} (C m^{-1})	σ (Ω^{-1})
96487	5F	10^{-8}

Table II.
OTHER IPMC PARAMETERS.

D_f	ε (mF m^{-1})	L_p	Y (GP$_a$)
3,35E-10	1,41	3,55E-6	1,79

The two IPMC actuators are rectangular and deformable surfaces. Both actuators have parts only made of Nafion, and other parts covered with platinum electrodes. These can be excited from separate current power sources, allowing independent actuation of each IPMC part with electrodes.

1) IPMC Actuator No. 1: Fig. 4(a) shows its geometry and dimensions. The actuator is made of Nafion partially covered with a central platinum electrode surface measuring 17 mm, and with both sides 1 and 3 made only of Nafion polymer. White regions in Fig. 4(a) are non-charged regions and the grey region is the charged one. The advantage of using a non-uniformly charged configuration for an IPMC actuator is the fact that the Nafion having a low Young modulus, this will allow larger actuator deformations when compared with IPMC actuators that are completely covered by an electrode layer.

To obtain the IPMC displacement using our model, we consider the actuator made of three modules that are serially connected (Fig. 4(b)). We attribute to each module a displacement variable (ξ_1, ξ_2 or ξ_3), and also its initial and final coordinate points (0, b_1, b_2 or b_3). To estimate the IPMC shape when an electric current is applied to its central electrode, the equation to be used is (33), assuming that there is no significant external pressure applied, $\Delta T_2 = 0$, and in the non-charged Nafion regions the electric current is zero, $i = 0$.

To calculate the constants in (33), boundary conditions of IPMC are examined. Since each actuator side is clamped, the displacement and flexion at these points is zero. Hence, we deduce relations (34), each for a boundary condition.

$$\xi_1(0) = \xi(\mathrm{b}_3) = 0 \quad , \quad \frac{d\xi_1(0)}{dx_1} = \frac{d\xi(\mathrm{b}_3)}{dx_1} = 0 \,. \tag{34}$$

Other boundary conditions are located at the interfaces between charged and non-charged regions, marked in Fig. 4(b) with b_1 and b_2 coordinates. In each interface, the displacement and its derivative must be equal for both sides of the piece. Therefore, we have relations (35).

$$\xi_1(b_1) = \xi_2(b_1)\,, \frac{d\xi_1(b_1)}{dx_1} = \frac{d\xi_2(b_1)}{dx_1}\,, \xi_2(b_2) = \xi_3(b_2)\,,$$

$$\frac{d\xi_2(b_2)}{dx_1} = \frac{d\xi_3(b_2)}{dx_1} \tag{35}$$

Finally, mechanical stresses $T_{11}{}^{mec}$ and $T_{12}{}^{mec}$ on each side of the interfaces must be equal. Thus, one gets (36).

$$T_{11}^1 = -T_{11}^2\,,\; T_{12}^1 = -T_{12}^2\,,\; T_{11}^2 = -T_{11}^3\,,\; T_{12}^2 = -T_{12}^3 \tag{36}$$

Using all boundary conditions in (33) to calculate each constant, the displacement equation was determined for each module of the IPMC actuator.

Model validation with IPMC actuator No. 1 is shown in Fig. 5. Experimental data is represented by triangular markers (▲), the model shape prediction considering gravitation's effect by dotted line, and the model prediction without taking into account the gravitation force by solid line. Figure 5 shows the actuator displacement ξ when an electric current *i* of 0.5 mA was applied in the central and charged area of the IPMC.

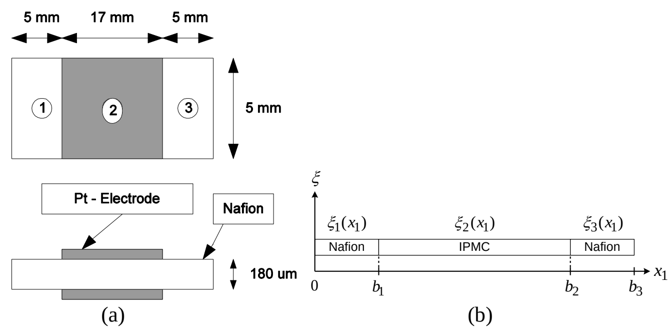

Fig. 4. (a) Non-uniformly charged IPMC No. 1: sheet geometry and dimensions. (b) Coordinate axis x_1 and ξ, displacement variables ξ_1, ξ_2 and ξ_3, and interface points b_1 and b_2 of IPMC actuator No. 1.

One verifies in Fig. 5 that the prediction of the model without gravitation force's effect gives results higher than those ones obtained with the model, which takes into account the gravitation force. However, due to the small dimensions of this IPMC piece and thus the quantity of electrolyte absorbed by the IPMC, the model results without gravitation when compared with those ones considering gravitation, they do not show large differences between their displacement values. Since the IPMC length is short, gravity effects are not dominant in this piece.

The model with gravitation however predicts displacements closer to the experimental ones in Fig. 5, showing the good performance of the proposed model including gravity. The largest disagreements between the experimental and the model with gravitation results are caused by breakable electrode material that was appearing in actuator surface due to its use, which introduced internal stresses deforming the IPMC shape.

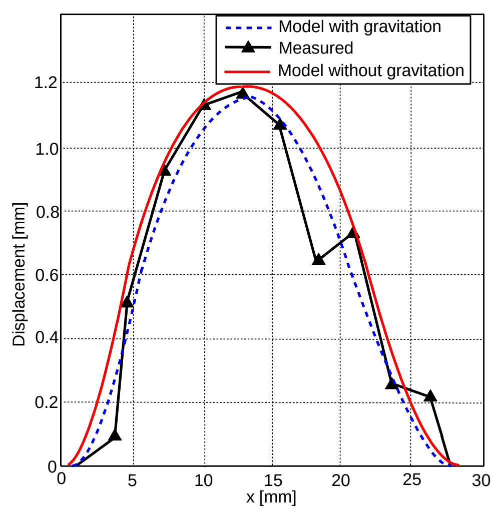

Fig 5. Comparison between model with and without gravitation, and real displacements for IPMC No. 1 under 0.5 mA applied to its central electrode.

2) IPMC Actuator No. 2: Fig. 6 shows the second non-uniformly charged IPMC actuator. It has a rectangular shape with a series of intercalated charged (grey colour) and non-charged (white colour) regions. Fig. 7 shows a photo of the IPMC actuator clamped at its start and its end. This actuator is particularly interesting since we can change its shape by choosing which electrodes are electrically excited. In Fig. 8, we show a general view of the experimental setup used to test the IPMC actuator No. 2. The picture shows the laser position sensor placed above the actuator to measure its displacement in several points. The electric wires, soldered in each electrode layer, are indicated in Fig. 8, where one can choose which electrodes will be connected to the current power source using the connectors shown in the bottom of the picture.

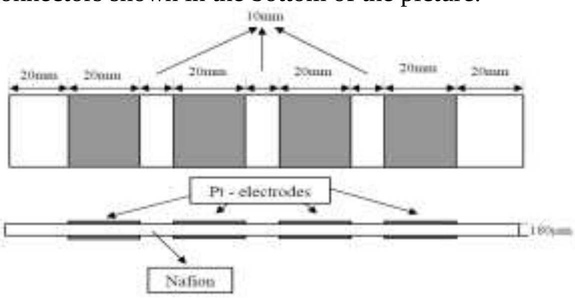

Fig 6. IPMC No. 2: intercalated charged non-charged areas and dimensions.

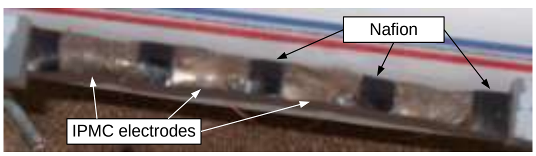

Fig 7. Illustration of the electric wire soldering in each platinum electrode.´

A series of experimental tests were made with this actuator to produce different shapes by energizing different sets of electrodes. Simulations were also effectuated using the model developed. For each simulating case, one sets first the electric current constant value. Follow, using Eqs. (25) to (30) and Eq.(110) of [26], the steady-state induced voltage V at IPMC terminals is obtained. This voltage is the electric excitation used in the electromechanical Eq. (33) to obtain the IPMC displacement. Fig. 9(a) presents the first test where all four actuator electrodes were energized. Three different constant electric currents were applied: 10 mA, 27.8 mA, and 42.3 mA. The steady-state and constant voltage value that appeared at the IPMC after 10s is shown in Fig. 9(a) for each electric current. The figure also shows the measured actuator displacements (triangle marks ▲) and the model results (dotted lines) for each electric current value, thus showing the shapes produced. Note that the actuator inflates as the electric current value becomes higher. The model also shows a symmetric inflation for all current values. However, this symmetry is only shown by the measured results with currents 10 mA and 27.8 mA. For 42.3 mA, the actuator has low displacement values in its right side. We verified that this asymmetric behaviour came from the flexibility and breakable characteristics shown by the platinum layer, which appeared considerable in the rightmost platinum electrode of the actuator during our experiments.

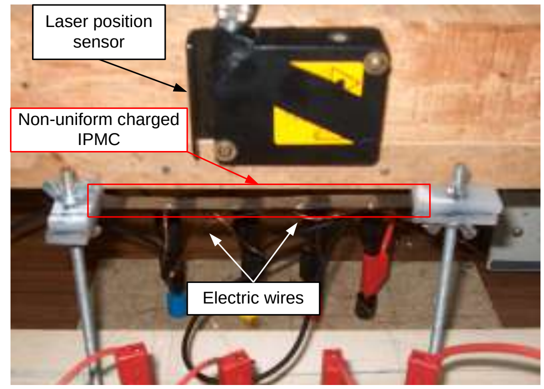

Fig 8. Setup with laser sensor, clamped IPMC, and electric wires.

To change the actuator shape again, we made a second test where only the two leftmost electrodes were energized by the same electric current. Fig. 9(a) shows how the IPMC shape changes for three different currents: 35 mA, 50 mA, and 59 mA. As current increases, the left side of the actuator inflates more and more, with the model following the experimental results with good accuracy. The maximum displacement achieved was about 5.4 mm.

In a third and interesting test, we repeated the previous procedure but now inverting the sign of the electric current. As shown by Fig. 11(a), the actuator moves down its left side. We used four different current values: 10 mA, 24.3 mA, 30 mA, and 53 mA. Compared with the previous results in Fig. 10(a), the actuator achieves now larger displacements. For example, the maximum downward displacement achieved was about 8.5 mm. This occurs because now we have a significant effect due to gravity's acting on the IPMC actuator, which has a considerable length (150 mm). The same consequences are revealed by the model results because it has now incorporated the gravitation force.

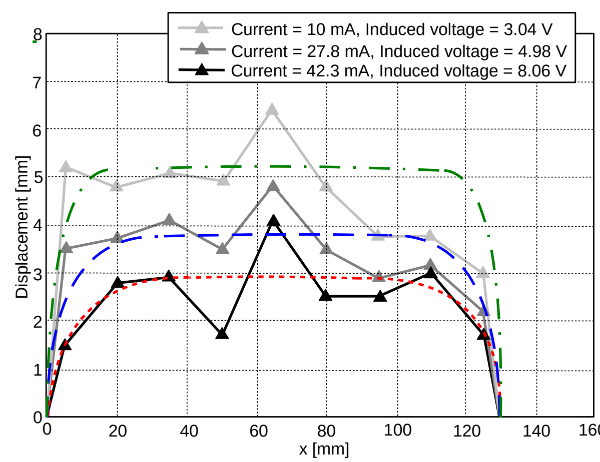

(a)

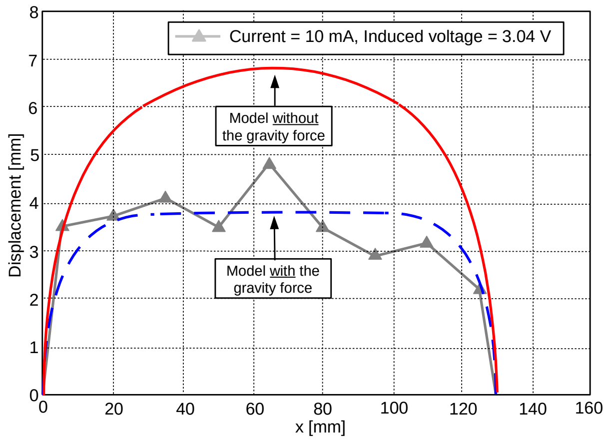

(b)

Fig 9. (a) First experimental and model gravitation's force results. Electrodes energized with different electric currents: 10.0, 27.8, and 42.3 mA. (b) Models with and without gravitation, energized with 10 mA.

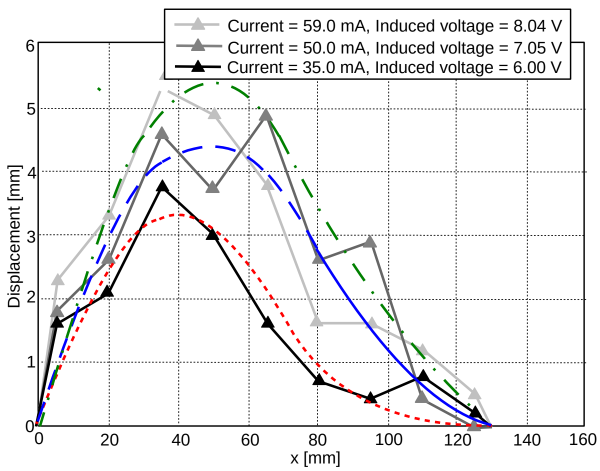

(a)

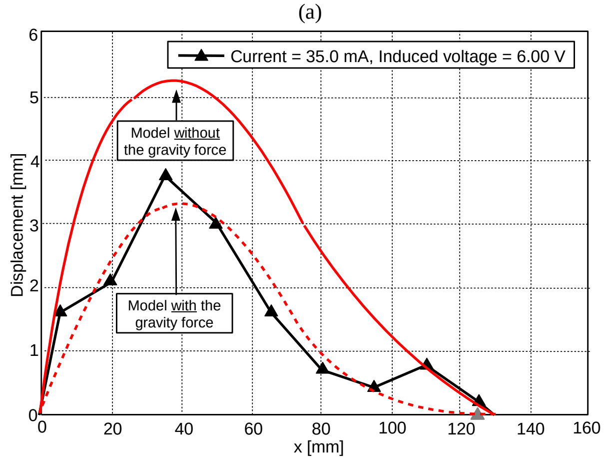

(b)

Fig 10. (a) IPMC displacement when only two leftmost electrodes are energized for currents: 35.0, 50.0, and 59 mA. (b) Comparison between models with and without gravitation's force, energized with 35 mA.

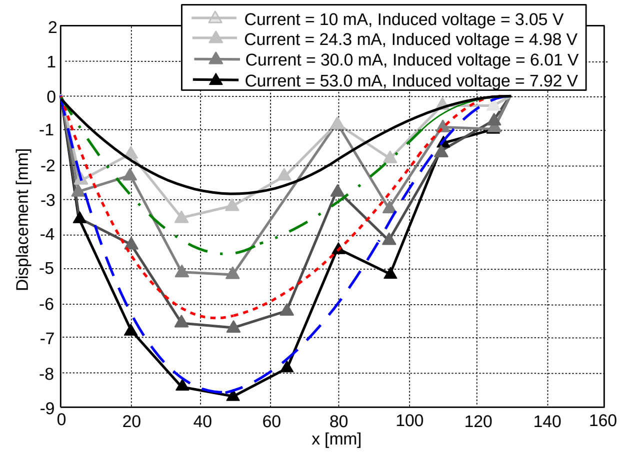

(a)

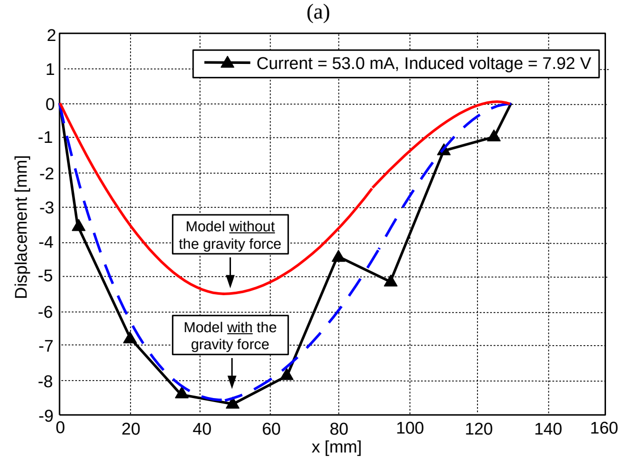

(b)

Fig 11. (a) IPMC downward displacement with two leftmost electrodes negatively energized: -10.0, -24.3, -30.0, and -53.0 mA. (b) Models with and without gravitation's force, energized with 53 mA.

Figs. 9(b), 10(b) and 11(b) compared the model results when considering the gravitation's force and when not considering it. Contrary to the results in Fig. 5, the IPMC has now a large dimension enough to the gravitation's force to be dominant for a correct prediction of an IPMC shape.

The experimental results in Fig. 9(b) clearly show that the IPMC acquires a central flat shape due to the gravity effect when energized. The same is predicted by our model when the gravitation's force is considered. However, when neglecting the gravity in the model, this shows in Fig. 9(b) a round shape instead a flat one, resulting in a very wrong prediction of the IPMC displacements. Similar results and conclusions can be inferred from Fig. 10(b) where only the most left IPMC electrodes were energized.

In Fig. 11(b), the conditions are the opposite of those in Fig. 10(b). The IPMC was now energized to be pushed down in the same direction of the gravitation's force. Considering the gravity effect in the model, this presents a very good prediction of the IPMC shape. However, when the gravity is not taken into account, the model lacks accuracy, showing displacements far enough of the real ones.

IV. Conclusion

In this paper, an electromechanical model that takes into account the effect of the gravitation force for large and hydrated IPMC actuators was developed to model non-uniformly charged IPMCs. To validate the model, two non-uniformly charged IPMC actuators were built and a number of experimental results were presented. The good agreement between model predictions and experimental results revealed the usefulness of the model developed in the electromechanical characterization of the new non-uniformly charged IPMC actuators.

References

[1] C. Lim, I-M. Chen, L. Yan, G. Yang, and K.-M. Lee, "Electromechanical Modeling of a Permanent-Magnet Spherical Actuator Based on Magnetic-Dipole-Moment Principle," *IEEE Transactions on Industrial Electronics*, vol. 56, no. 5, pp. 1640–1648, May 2009.

[2] K. Takahashi, E. Bulgan, Y. Kanamori, and K. Hane, "Submicrometer Comb-Drive Actuators Fabricated on Thin Single Crystalline Silicon Layer," *IEEE Transactions on Industrial Electronics,* vol. 56, no. 4, pp. 991–995, Apr. 2009.

[3] A. Khaligh, P. Zeng, and C. Zheng, "Kinetic Energy Harvesting Using Piezoelectric and Electromagnetic Technologies—State of the Art," *IEEE Transactions on Industrial Electronics,* vol. 57, no. 3, pp. 850–860, Mar. 2010.

[4] T. Higuchi, K. Suzumori, and S. Tadokoro, eds, *Next-Generation Actuators Leading Breakthroughs*, Berlin: Springer, 2010.

[5] A. Bellini, M. Colli, and E. Dragoni, "Mechatronic Design of a Shape Memory Alloy Actuator for Automotive Tumble Flaps: A Case Study," *IEEE Transactions on Industrial Electronics,* vol. 56, no. 7, pp. 2644–2656, Jul. 2009.

[6] W.-J. Kim and A. Sadighi, "A Novel Low-Power Linear Magnetostrictive Actuator With Local Three-Phase Excitation," *IEEE/ASME Transactions on Mechatronics,* vol. 15, no. 2, pp. 299–307, Apr. 2010.

[7] K. Tsiakmakis, J. Brufau-Penella, M. Puig-Vidal, and T. Laopoulos, "A Camera Based Method for the Measurement of Motion Parameters of IPMC Actuators," *IEEE Transactions on Instrumentation and Measurement,* vol. 58, no. 8, pp. 2626–2633, Aug. 2009.

[8] P. Brunetto, L. Fortuna, P. Giannone, S. Graziani, and F. Pagano, "A Resonant Vibrating Tactile Probe for Biomedical Applications Based on IPMC," *IEEE Transactions on Instrumentation and Measurement,* vol. 59, no. 5, pp. 1453–1462, May 2010.

[9] M. Shahinpoor and H.-J. Schneider, eds, *Intelligent Materials*, Royal Society of Chemistry Publishers, 2008.

[10] F. Carpi, C. Menon, and D. De Rossi, "Electroactive Elastomeric Actuator for All-Polymer Linear Peristaltic Pumps," *IEEE/ASME Transactions on Mechatronics,* vol. 15, no. 3, pp. 460–470, Jun. 2010.

[11] F. Carpi, G. Frediani, and D. De Rossi, "Hydrostatically Coupled Dielectric Elastomer Actuators," *IEEE/ASME Transactions on Mechatronics,* vol. 15, no. 2, pp. 308–315, Apr. 2010.

[12] M. Shahinpoor and K. J. Kim, "Ionic Polymer-Metal Composites – III. Modeling and Simulation As Biomimetic Sensors, Actuators, Transducers and Artificial Muscles", *Smart Materials and Structures*, vol. 13, no. 4, pp. 1362–1388, 2004.

[13] K. Kikuchi, S. Tsuchitani, "Nafion-based polymer actuators with ionic liquids as solvent incorporated at room temperature," *Journal of Applied Physics*, vol. 106, no. 5, pp. 053519-053519-8, Sep. 2009

[14] S. Kim, C. Cho, and Y. Kim, "Polymer packaging for arrayed ionic polymer–metal composites and its application to micro air vehicle control surface", *Smart Materials and Structures,* vol. 18, no. 11, pp. 115009, 2009.

[15] J. Barramba, J. Silva, and P.J. Costa Branco, "Evaluation of dielectric gel coating for encapsulation of ionic polymer-metal composite (IPMC) actuators," *Sensors Actuators* A vol. 140, pp. 232–8, 2007.

[16] D. Pugal, K. Jung, A. Aabloo, and K. J. Kim, "Ionic polymer-metal composite mechanoelectrical transduction: review and perspectives," *Polymer International*, vol. 59, no. 3, pp. 279–289, 2010.

[17] B. Lopes and P. J. Costa Branco, "Ionic polymer metal-composite (IPMC) actuators: Augmentation of their actuation force capability," in *IECON '09. 35th Annual Conference of IEEE,* 3–5 Nov. 2009, *Industrial Electronics, 2009*, , no. , pp. 1180–1184.

[18] W. Robinson, *Charge control of ionic polymer*s, Master Thesis, Virginia Polytechnic Institute and State University, USA, 2005.

[19] P. J. Costa Branco and J. Dente, "Derivation of a continuum model and its electric equivalent-circuit representation for the ionic polymer metal composite (IPMC) electromechanics," *Smart Materials and Structures*, vol. 15, pp. 378–392, 2006.

[20] Y.Nakabo et al., "Kinematic modeling and visual sensing of multi-DOF robot manipulator with patterned artificial muscle, *Proceedings of the 2005 IEEE International Conference on Robotics and Automation*, pp. 4326-4331, 2005.

[21] K.J.Kim et al., "Ionic Polymer-metal Composites for Underwater Operation", *Journal of Intelligent Materials Systems and Structures*, vol. 13, pp.123-131, 2007.

[22] D.Dogruer et al., "Fluid interaction of segmented ionic polymer-metal composites under water", *Smart Materials and Structures*, vol. 16, pp. S220-S226, 2007.

[23] A.J. McDaid et. al., "A conclusive scalable model for the complete actuation response for IPMC transducers," *Smart Materials and Structures,* vol. 19, 075011, 2010.

[24] J. Santos, B. Lopes, and P.J. Costa Branco, "Ionic Polymer-Metal Composite Material as a Diaphragm for Micropump Devices", *Sensors and Actuators* A: Physical, 2010.

[25] H.H. Woodson and J.R. Melcher, *Electromechanical Dynamics. Part III. Elastic and Fluid Media,* New York: Wiley, 1968.

[26] S. Nair, *Introduction to Continuum Mechanics,* Cambridge Univ. Press, 2009.

[27] W. Reynolds, *Thermodynamics,* New York: McGraw-Hill, 1968.

P. J. Costa Branco (M'91) is currently an Associate Professor at the Department of Electrical and Computing Engineering, Scientific Area of Energy, Instituto Superior Técnico (IST), Lisbon, Portugal. His research areas are in electrical machines, control of electrical drives, and he is presently engaged in research on advanced actuators/sensors based on smart materials as piezoelectric, ionic polymers and superconductors.

J. A. Dente graduated in electrical engineering and received the Ph.D. degree in electrical engineering from the Instituto Superior Técnico (IST), Lisbon, Portugal, in 1975 and 1986, respectively. From 1989 to 1993, he was an Associate Professor at IST, where he is currently a Full Professor in the area of electrical machines in the Department of Electrical and Computing Engineering, Scientific Area of Energy. His primary areas of interest are in electrical machines, motion control, and he presently is engaged in research on electrical generators for wave and wind energy converters.

B. Lopes graduated in electrical engineering and received the Master Degree in electrical engineering from the Instituto Superior Técnico (IST), Lisbon, Portugal, in 2009. From 2009 he is with EDP working in the area of Chemical Industry Planning.